Original Article

Glial Cells and Retinal Nerve Fibers Morphology in the Optic Nerves of Streptozotocin-induced Hyperglycemic Rats

Rafael Aleman-Flores, MD, PhD; Blanca Mompeo-Corredera, MD, PhD

Department of Morphology, University of Las Palmas de Gran Canaria, Spain

Abstract

Purpose: This study analyzes the structures of optic nerve elements, i.e., glial cells and nerve fibers, in an STZ-induced hyperglycemic animal model. Morphological changes in glial elements of the optic nerve in hyperglycemic and normoglycemic animals were compared.
Methods: Transmission electron microscopy, histochemistry, immunohistochemistry, and morphometry were used in this study.
Results: Hyperglycemia increased the numbers of inner mesaxons and axons with degenerative profiles. Furthermore, it led to both an increase in the amount of debris and in the numbers of secondary lysosomic vesicles in glial cytoplasm. Hyperglycemia also led to a decrease in glial fibrillary acidic protein expression and an increase in periodic acid-Schiff-positive deposits in the optic nerves of hyperglycemic animals.
Conclusion: We conclude that the damage to the structural elements observed in our animal models contributes to the pathogenesis of optic neuropathy in the early stages of diabetes.

Keywords: Hyperglycemia; Model Animal; Myelin Sheath; Neuroglia; Optic Nerve; Optic Nerve Disease

J Ophthalmic Vis Res 2018; 13 (4): 433-438

INTRODUCTION

Diabetic ophthalmopathy is one of the most common chronic complications of diabetes mellitus, and includes ocular pathologies such as cataract, glaucoma,[1,2] diabetic retinopathy, and optic neuropathy.[2] Diabetic retinopathy is a major complication of diabetes. Although diabetic retinopathy was previously considered to have a vascular origin, it is now recognized as a neuro-vascular disease.[3,4]

Correspondence to:
Blanca Mompeo-Corredera, MD, PhD. Department of Morphology, Faculty of Health Sciences. C/Blas Cabrera Felipe s/n 35016 Las Palmas de Gran Canaria, Spain.
E-mail: blanca.mompeo@ulpgc.es

Received: 13-08-2017 Accepted: 16-06-2018

Access this article online

Quick Response Code:

Website: www.jovr.org

DOI: 10.4103/jovr.jovr_130_17

Cellular and molecular studies in retinas of hyperglycemic experimental animals suggest that neurons are vulnerable to hyperglycemia and are damaged shortly after the onset of the disease before any signs of vascular damage.[3,4] Diabetic optic neuropathy is a clinical condition involving the optic pathway. It may be asymptomatic and can only be detected using electrophysiological measurements.[5] This pathology, which has not been deeply studied, might develop in the absence of diabetic retinopathy. Although some morphological and morphometric studies have been performed in the optic nerve in the presence of hyperglycemia,[6-9] there are many unanswered questions in this area of research. In this study, we describe the structural characteristics of glial cells in the optic nerves

How to cite this article: Aleman-Flores R, Mompeo-Corredera B. Glial cells and retinal nerve fibers morphology in the optic nerves of streptozotocin-induced hyperglycemic rats. J Ophthalmic Vis Res 2018;13:433-8.

of streptozotocin (STZ)-induced hyperglycemic model rats and the relationships among these characteristics and damaged nerve fibers.

METHODS

Animals and Treatment of Samples

Healthy two-month-old Sprague Dawley rats (n = 72) with body weights of 263 ± 58.65 g were randomly assigned into a diabetic (n = 36) or control (n = 36) group. Hyperglycemia was induced in the diabetic group by a single intraperitoneal injection of STZ (65 mg/kg) in citrate buffer, pH 4.5. The control group of animals only received a buffer injection. The diabetic animals did not receive insulin to correct the hyperglycemia. A blood glucose level higher than 200 mg/dl was the criterion for inclusion in the hyperglycemic group. Glucose levels in plasma were assessed weekly. Animals were maintained on a 12-hr light-dark cycle with standard food and water available *ad libitum*. Eighteen hyperglycemic and 18 control animals were sacrificed six and 12 weeks after the STZ or buffer injection. The animals were anesthetized with an intraperitoneal injection of Equithesin® (3.3 ml/kg; 9.5 mg pentobarbital sodium, 76 ml ethanol, 42.5 mg chloral hydrate, 428 mg propylene glycol, 21 mg magnesium sulfate, and distilled water up to 1 ml). The animal experiments followed the Animal Research: Reporting of *In Vivo* Experiments guidelines. They were carried out in accordance with the UK. Animals (Scientific Procedures) Act, 1986, and the associated guidelines, the EU Directive 2010/63/EU for animal experiments, and the guidelines of RD 1201/2005 (Spain) on the protection of animals used for research and other scientific purposes.

Tissue Preparation and Histopathology

The animals were transcardially perfused with a physiological saline solution prior to fixation. Two types of fixative were used: 2% glutaraldehyde solution in 0.1 M phosphate buffer, pH 7.4; and 4% paraformaldehyde solution. The fixative was selected based on whether the samples were allocated for ultrastructural studies or for studies requiring paraffin embedding, respectively. Thirty hyperglycemic and 30 control animals were used for ultrastructural studies, and six hyperglycemic and six control animals were used for studies requiring paraffin embedding. The optic nerves were extracted through craniotomies and preserved in the same fixative utilized for perfusion. A 2-mm segment of the right nerve, just before the chiasm, was used for this study.

Agar 100-embedded samples

Specimens for transmission electron microscopic observation were post-fixed in 1% OsO_4, dehydrated in ethanol, and embedded in Agar 100 resin using a routine lab technique.[6,8] Semi-thin and ultra-thin sections were obtained using an ultramicrotome (Ultracut S, Reichert®, Austria). One micrometer-thick sections were stained with toluidine blue for light microscopic observation. Ultra-thin 500-600-Å sections were counterstained with uranyl and lead citrate using the method described by Reynolds (1963)[10] and observed using a Phillips 301 transmission electron microscope (Holland). Several ultrathin sections from the 30 hyperglycemic animals (6 and 12 weeks post-STZ injection) and the 30 control animals (6 and 12 weeks post-buffer injection) were observed by transmission electron microscopy.

Paraffin-embedded samples

Specimens used for the assessment of periodic acid-Schiff (PAS)-positive deposits and glial fibrillary acidic protein (GFAP) immunodetection were embedded in paraffin and cut into 5-µm-thick sections. Following deparaffinization and hydration, the sections were subjected to routine staining for PAS or processed for immunohistochemical detection of GFAP according to the protocol provided with the GFAc.Prot home kit (Sigma-Aldrich®, San Luis, Missouri, USA).

Morphometry

All myelinated and unmyelinated nerve fibers were counted in images from ten random areas of semi-thin sections obtained from each nerve (9,800X magnification). Thirty nerves from hyperglycemic animals and 30 control nerves were used in this morphometric study. No masking was used. The diameters of both axons and fibers in each image were measured using an image analyzer (Image Pro v6.0, Media Cybernetics®, Maryland, USA). The thicknesses of the myelin sheaths were estimated based on these measurements.

Statistical Analysis

The means and standard deviations of the measurements were calculated. When two conditions were considered, the Mann-Whitney test was used. Statistical analysis was performed the computer software IBM-SPSS Statistics 24 (USA). The level of significance considered was $P \leq 0.05$.

RESULTS

Animals

STZ-induced hyperglycemic animals had smaller weight gains than control animals 6 and 12 weeks post-injection [Table 1]. The level of glucose was significantly higher in hyperglycemic animals, 30% of which had a glucose level between 300 and 320 mg/ml,

and 70% of which had a glucose level higher than 500 mg/ml.

Structures and Ultrastructures of Nerve Fibers

In control animals, myelinated and unmyelinated fibers formed fascicles shared with glial cell processes and blood vessels. The axoplasms of the fibers were light and contained mitochondria, microtubules, and neurofilaments. Mesaxon structures were not frequently found at the ages studied [Figure 1a]. In the hyperglycemic animals, many of the fibers did not show morphological damage. However, some axons had swollen mitochondria and vesicular bodies without other apparent changes in the cytoskeletal composition. In addition, a considerable number of axons were surrounded by an inner mesaxon structure. Myelin collapse and lamellar membranous bodies were also frequently observed in hyperglycemic animals [Figure 1b-f].

Table 1. Animal weights during the study

Animal weights (g)	C6	HG6	C12	HG12
Initial weight (g)	263.33±66.15	263.33±64.08	271.66±64.70	254.16±39.67
Final weight (g)	363.66±91.20	233.33±88.75	377.16±99.27	199.16±56.07
Variation (%)	+38.1	−11.39*	+38.8	−24.26*

C6, control animals (6 weeks postbuffer injection); C12, control animals (12 weeks postbuffer injection), HG6, hyperglycemic animals (6 weeks post-STZ injection); HG12, hyperglycemic animals (12 weeks post-STZ injection); STZ, streptozotocin

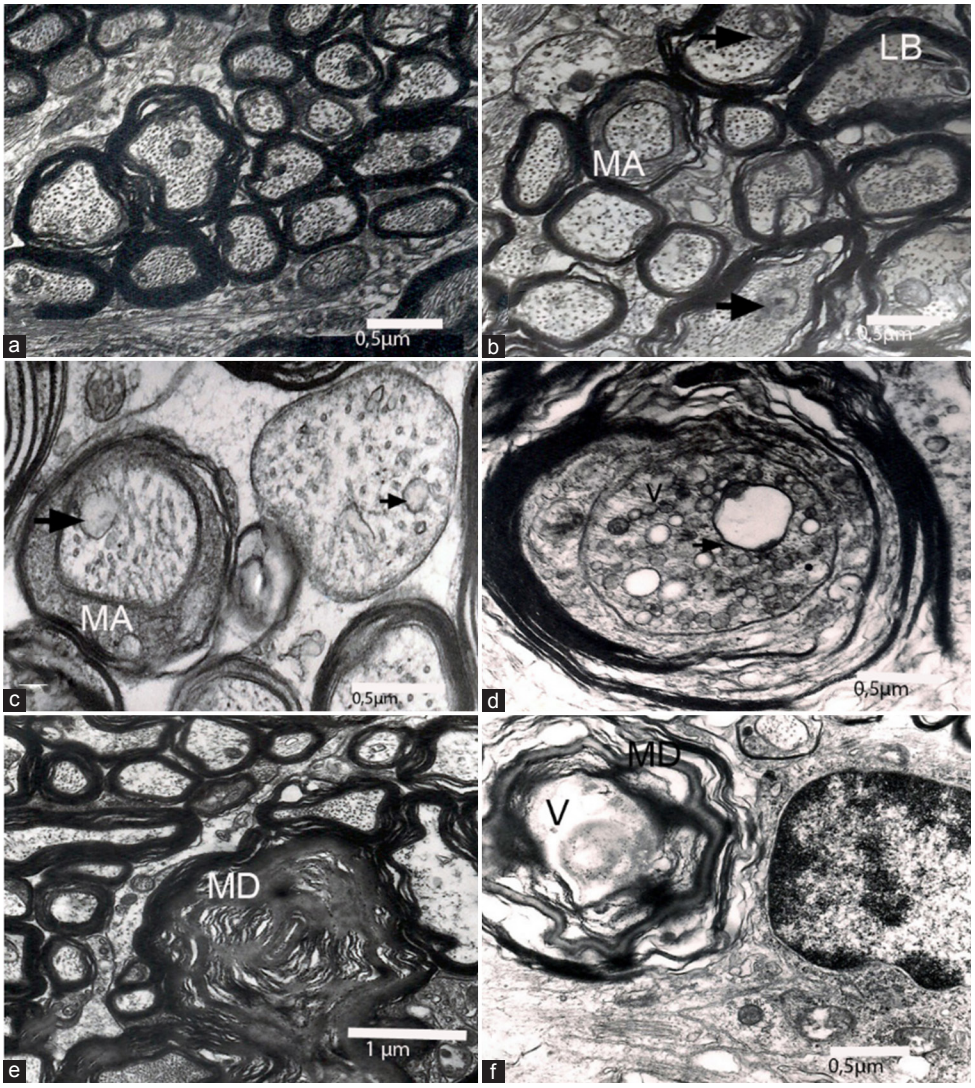

Figure 1. Nerve fibers of the optic nerve. (a) Control rat. Note the well-preserved myelinated fibers. (b-d) Hyperglycemic animals. Note the presence of mesaxon structures, the swollen mitochondria (arrows), and the degenerating fibers (V). (e and f) some axons are missing and the myelin sheaths are collapsed in other axons.

Morphometric Parameters

In healthy animals, 1.97% of the fibers were unmyelinated, while 1.38% of the fibers remained unmyelinated in the STZ-induced hyperglycemic animals 6 and 12 weeks post-STZ injection. There were no statistically significant differences between the two groups.

We observed no changes in the myelin thickness of nerve fibers 6 weeks post-STZ injection. However, we observed slightly thinner myelin in the hyperglycemic animals than in control animals 12 weeks post-injection. These differences were not statistically significant [Table 2].

Table 2. Thickness of the myelin sheath

Myelin thickness of the myelinated fibers	C6	HG6	C12	HG12
Myelin thickness (μm)	0.36±0.2	0.36±0.25	0.53±0.25	0.48±0.22

C6, control animals (6 weeks postbuffer injection); C12, control animals (12 weeks postbuffer injection); HG6, hyperglycemic animals (6 weeks post-STZ injection); HG12, hyperglycemic animals (12 weeks post-STZ injection); STZ, streptozotocin

Structures of Glial Cells and their Disposition in the Optic Nerve

Glial cells were distributed throughout the optic nerve. Astrocytic processes were found surrounding groups of fibers. The astrocytes contacted the surfaces of the nerve and the perivascular spaces, forming perivascular astrocyte end-feet.

Periodic Acid-Schiff -positive Deposits in the Nerve

In control animals, scarce deposits of PAS-positive material were observed throughout the nerve. In hyperglycemic animals there were abundant deposits in the extracellular space, inside cellular glial bodies and around the microvessels [Figure 2a and b]. Additionally, there was an increase in the number of PAS-positive deposits from 6 to 12 weeks after the STZ injection.

Glial Fibrillary Acidic Protein in the Nerve

GFAP was detected in fibrous astrocytes. GFAP-positive processes were mostly located in perivascular spaces, the nerve periphery, and within groups of nerve fibers [Figure 2c]. Six weeks post-STZ injection, GFAP appeared mostly in astrocytes in perivascular spaces and the periphery of the nerve. However, there was a decrease in GFAP expression in astrocytes located among the groups of nerve fibers. GFAP expression was less intense 12 weeks post-STZ injection [Figure 2d].

Ultrastructural Analysis

Astrocytes in healthy optic nerves had abundant cytoplasm and a light nucleus with heterochromatin located under the periphery of the nucleus. The cytoplasm contained some lipid droplets and numerous filaments, mainly in the astrocytic processes. The gap junctions between astrocytes were preserved [Figure 3a]. Oligodendrocytes had rounded nuclei with punctate chromatin. These cells had cytoplasms that were rich in mitochondria and microtubules with a well-developed Golgi apparatus and endoplasmic reticulum [Figure 3b]. Six weeks post-STZ injection, the cytoplasms of astrocytes

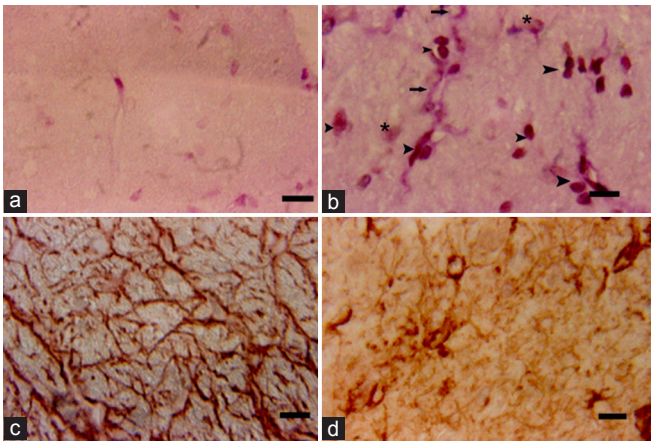

Figure 2. Periodic acid-Schiff-positive staining (a and b) and glial fibrillary acidic protein expression (c and d) in the optic nerves of control and hyperglycemic animals. Bar = 10 μm. Periodic acid-Schiff staining in the optic nerve of a control animal (a) and that of a hyperglycemic animal (b). Note the localization of periodic acid-Schiff-positive deposits in cellular bodies (arrowhead), cellular processes (arrows), and the extracellular space (*). Glial fibrillary acidic protein expression in a control optic nerve (b) and an optic nerve from a hyperglycemic animal (d). Note the loss of glial fibrillary acidic protein in the astrocytic processes of hyperglycemic animals.

contained secondary lysosomes and lamellar bodies. Intermediate filaments seemed to be few in hyperglycemic animals compared to the control group [Figure 3c]. The oligodendrocytes had active cytoplasmic organelles such as dilated Golgi saccules, endoplasmic reticulum, and cytoplasmic lamellar crystalloid bodies [Figure 3d]. Twelve weeks post-STZ injection, some glial cells had increased numbers of crystalloid lamellar bodies and debris in their cytoplasms. Some of these cells had degenerative cellular features and pyknotic nuclei with condensed chromatin [Figures 3e and f].

DISCUSSION

STZ-induced hyperglycemia has been shown to be a reliable experimental model to study the effects of hyperglycemia in the optic pathway. In this model, we previously observed changes in the blood-brain barrier[8] and the loss of larger fibers in the optic nerve.[6] In the present observational study of the cellular components

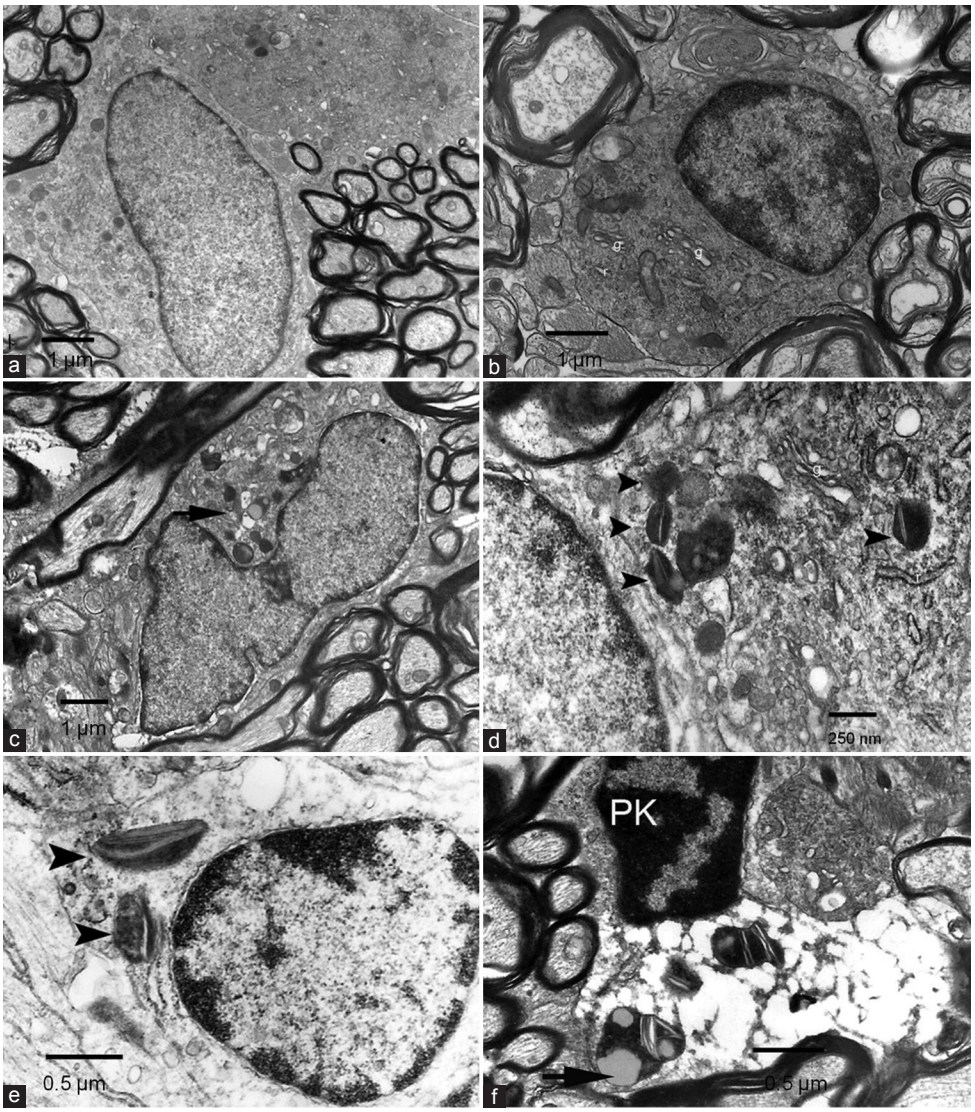

Figure 3. Glial cells in control group: astrocyte (a), oligodendrocyte (b). Glial cells in hyperglycemic group (d-f). Note the presence of secondary lysosomes (arrows) and crystalloid inclusions in the cytoplasms of glial cells (arrowheads). Panel f shows a pyknotic nucleus and degradation of the cytoplasm. m, mitochondria; g, Golgi saccules; r, endoplasmic reticulum and ribosomes.

of the optic nerve, we observed changes in glial cells associated with the hyperglycemic condition. We found: (1) presence of cytoplasmic secondary lysosomes and some myelin debris in the cytoplasm, (2) loss of GFAP expression in astrocyte processes, and (3) carbohydrate deposits located inside the cells and in the extracellular space.

Although many of the glial components remained unaffected in the hyperglycemic animals, the presence of the affected cells was not infrequent six or twelve weeks post STZ-injection. The affected cells were always observed in the ultrastructural transmission electron micrographs at low magnification. This condition was not present in the control samples. Future morphometric studies could overcome the quantitative limitations of this preliminary qualitative observational study.

The presence of secondary lysosomes could be related to the damaged and missing fibers, which have been previously observed in optic nerves from hyperglycemic animals.[6] An initial disconnection between the myelin sheath and the affected axon would explain the considerable numbers of inner mesaxon structures, which were observed in the optic nerves from hyperglycemic animals.

Lamellar crystalloid formations in glial cells have been reported to be related to decreased autophagocytic activity in experimental diabetes. Hyperglycemia may be associated with reduced autophagy, which would lead to protein aggregation and accumulation of dysfunctional organelles.[11-13] Decreased autophagy, among other pathological processes, has thus been implicated in the pathogenesis of cardiac dysfunction due to hyperglycemia.[12]

The presence of PAS-positive deposits in the central nervous system (CNS) as a consequence of neurodegenerative disorders and aging has been demonstrated.[14,15] PAS-positive staining has been observed in extracellular spaces, glial cells, and neurons in experimental models. PAS-positive deposits are located near edematous tissue, reactive astrocytes, proliferating microglia, dying neurons, and areas of compromised blood-brain barrier.[16] In our study, we demonstrated the presence of PAS-positive deposits in the optic nerves of hyperglycemic animals in the extracellular space, glial cells bodies, and cellular processes. These results support the idea that hyperglycemia may play an important role in the damage to the optic nerve by influencing local carbohydrate metabolism.

Some pathological conditions in the CNS including infection, inflammation, ischemia, trauma, tumors, and neurodegenerative diseases lead to the adoption of a reactive phenotype by astrocytes, which is associated with increased GFAP expression.[17,18] However, the situation seems to be different under hyperglycemic conditions. GFAP expression was lower in astrocytes in hyperglycemic animals compared to control animals. This fact supports the statement that hyperglycemia does not lead to reactive astrocytosis in the optic nerve. This statement is supported by different studies[19-23] reporting decreased astrocytic GFAP expression in the brain in hyperglycemic and experimental ischemic brain conditions.[24] The results of the above studies suggest that the effects of the hyperglycemic condition on astrocytes occur prior to the effects of experimental ischemia. Our findings about STZ-induced hyperglycemic animals may contribute to the understanding of pathogenesis of optic neuropathy in diabetes.

Financial Support and Sponsorship

Nil.

Conflicts of Interest

There are no conflicts of interest.

REFERENCES

1. Cairncross JP, Steinberg WJ, Labuschagne MJ. Prevalence of eye pathology in a group of diabetic patients at national district hospital outpatient department in bloemfontein, South Africa. *Afr J Prim Health Care Fam Med* 2017;9:e1-e7.
2. Khan A, Petropoulos IN, Ponirakis G, Malik RA. Visual complications in diabetes mellitus: Beyond retinopathy. *Diabet Med* 2017;34:478-484.
3. Lieth E, Barber AJ, Xu B, Dice C, Ratz MJ, Tanase D, et al. Glial reactivity and impaired glutamate metabolism in short-term experimental diabetic retinopathy. Penn state retina research group. *Diabetes* 1998;47:815-820.
4. Barber AJ, Lieth E, Khin SA, Antonetti DA, Buchanan AG, Gardner TW, et al. Neural apoptosis in the retina during experimental and human diabetes. Early onset and effect of insulin. *J Clin Invest* 1998;102:783-791.
5. Wolff BE, Bearse MA Jr. Schneck ME, Barez S, Adams AJ. Multifocal VEP (mfVEP) reveals abnormal neuronal delays in diabetes. *Doc Ophthalmol* 2010;121:189-196.
6. Aleman-Flores R, Mompeo-Corredera B, Ortega-Santana F, Limiñana-Cañal JM, Castaño-Gonzalez I Optic nerve fibers and experimental diabetes. *Arch Soc Esp Oftalmol* 2000;75:315-320.
7. Zhao JP, Ma ZZ, Song C, Li XH, Li YZ, Liu YY, et al. Optic nerve lesions in diabetic rats: Blood flow to the optic nerve, permeability of micro blood vessels and histopathology. *Int J Ophthalmol* 2010;3:291-294.
8. Alemán R, Mompeó B, Castaño I. Streptozotocin-induced diabetes, and the optic nerve blood barrier. *Arch Soc Esp Oftalmol* 2016;91:170-176.
9. Fernandez DC, Pasquini LA, Dorfman D, Aldana Marcos HJ, Rosenstein RE. Early distal axonopathy of the visual pathway in experimental diabetes. *Am J Pathol* 2012;180:303-313.
10. Reynolds ES. The use of lead citrate at high pH as an electron-opaque stain in electron microscopy. *J Cell Biol* 1963;17:208-12.
11. Quan W, Lim YM, Lee MS. Role of autophagy in diabetes and endoplasmic reticulum stress of pancreatic β-cells. *Exp Mol Med* 2012;44:81-88.
12. Wang F, Jia J, Rodrigues B. Autophagy, metabolic disease, and pathogenesis of heart dysfunction. *Can J Cardiol* 2017;33:850-859.
13. Jung HS, Lee MS. Role of autophagy in diabetes and mitochondria. *Ann N Y Acad Sci* 2010;1201:79-83.
14. Akiyama H, Kameyama M, Akiguchi I, Sugiyama H, Kawamata T, Fukuyama H, et al. Periodic acid-Schiff (PAS)-positive, granular structures increase in the brain of senescence accelerated mouse (SAM). *Acta Neuropathol* 1986;72:124-129.
15. Manich G, Cabezón I, Augé E, Pelegrí C, Vilaplana J. Periodic acid-Schiff granules in the brain of aged mice: From amyloid aggregates to degenerative structures containing neo-epitopes. *Ageing Res Rev* 2016;27:42-55.
16. Bennett SA, Stevenson B, Staines WA, Roberts DC. Periodic acid-Schiff (PAS)-positive deposits in brain following kainic acid-induced seizures: Relationships to fos induction, neuronal necrosis, reactive gliosis, and blood-brain barrier breakdown. *Acta Neuropathol* 1995;89:126-138.
17. Pekny M, Nilsson M. Astrocyte activation and reactive gliosis. *Glia* 2005;50:427-434.
18. Sofroniew MV, Vinters HV. Astrocytes: Biology and pathology. *Acta Neuropathol* 2010;119:7-35.
19. Afsari ZH, Renno WM, Abd-El-Basset E. Alteration of glial fibrillary acidic proteins immunoreactivity in astrocytes of the spinal cord diabetic rats. *Anat Rec (Hoboken)* 2008;291:390-399.
20. Barber AJ, Antonetti DA, Gardner TW. Altered expression of retinal occludin and glial fibrillary acidic protein in experimental diabetes. The Penn State Retina Research Group. *Invest Ophthalmol Vis Sci* 2000;41:3561-3568.
21. Coleman E, Judd R, Hoe L, Dennis J, Posner P. Effects of diabetes mellitus on astrocyte GFAP and glutamate transporters in the CNS. *Glia* 2004;48:166-178.
22. Dennis JC, Coleman ES, Swyers SE, Moody SW, Wright JC, Judd R, et al. Changes in mitotic rate and GFAP expression in the primary olfactory axis of streptozotocin-induced diabetic rats. *J Neurocytol* 2005;34:3-10.
23. Lechuga-Sancho AM, Arroba AI, Frago LM, García-Cáceres C, de Célix AD, Argente J, et al. Reduction in the number of astrocytes and their projections is associated with increased synaptic protein density in the hypothalamus of poorly controlled diabetic rats. *Endocrinology* 2006;147:5314-5324.
24. Jing L, He Q, Zhang JZ, Li PA. Temporal profile of astrocytes and changes of oligodendrocyte-based myelin following middle cerebral artery occlusion in diabetic and non-diabetic rats. *Int J Biol Sci* 2013;9:190-199.